

Research Paper

GREENBURST: A commensal Fast Radio Burst search back-end for the Green Bank Telescope

Mayuresh P. Surnis^{1,2} , D. Agarwal^{1,2}, D. R. Lorimer^{1,2}, X. Pei³, G. Foster⁴, A. Karastergiou^{4,5,6}, G. Golpayegani^{1,2}, R. J. Maddalena⁷, S. White⁷, W. Armour⁸, J. Cobb⁹, M. A. McLaughlin^{1,2}, D. H. E. MacMahon⁹, A. P. V. Siemion^{9,10,11}, D. Werthimer⁹ and C. J. Williams⁴

¹Department of Physics and Astronomy, West Virginia University, P.O. Box 6315, Morgantown, WV 26506, USA, ²Center for Gravitational Waves and Cosmology, West Virginia University, Chestnut Ridge Research Building, Morgantown, WV 26505, USA, ³Xinjiang Astronomical Observatory, Chinese Academy of Sciences, Urumqi, Xinjiang 830011, China, ⁴Sub-Department of Astrophysics, University of Oxford, Denys Wilkinson Building, Keble Road, Oxford OX1 3RH, UK, ⁵Physics Department, University of the Western Cape, Cape Town 7535, South Africa, ⁶Department of Physics and Electronics, Rhodes University, P.O. Box 94, Grahamstown 6140, South Africa, ⁷Green Bank Observatory, P.O. Box 2, Green Bank, WV 24944, USA, ⁸OeRC, Department of Engineering Science, University of Oxford, Keble Road, Oxford OX1 3QG, UK, ⁹Department of Astronomy, University of California, Berkeley, 501 Campbell Hall #3411, Berkeley, CA 94720, USA, ¹⁰Radboud University, Nijmegen 6525 HP, The Netherlands and ¹¹SETI Institute, Mountain View, CA 94043, USA

Abstract

We describe the design and deployment of GREENBURST, a commensal Fast Radio Burst (FRB) search system at the Green Bank Telescope. GREENBURST uses the dedicated *L*-band receiver tap to search over the 960–1 920 MHz frequency range for pulses with dispersion measures out to 10^4 pc cm⁻³. Due to its unique design, GREENBURST is capable of conducting searches for FRBs when the *L*-band receiver is not being used for scheduled observing. This makes it a sensitive single pixel detector capable of reaching deeper in the radio sky. While single pulses from Galactic pulsars and rotating radio transients will be detectable in our observations, and will form part of the database we archive, the primary goal is to detect and study FRBs. Based on recent determinations of the all-sky rate, we predict that the system will detect approximately one FRB for every 2–3 months of continuous operation. The high sensitivity of GREENBURST means that it will also be able to probe the slope of the FRB fluence distribution, which is currently uncertain in this observing band.

Keywords: instrumentation: miscellaneous – radio continuum: transients

(Received 14 March 2019; revised 11 June 2019; accepted 27 June 2019)

1. Introduction

Fast Radio Bursts (FRBs) are characterised by their millisecond duration and radio-frequency dispersion that far exceeds that predicted to result from interactions with free electrons in the Milky Way (Lorimer et al. 2007; Thornton et al. 2013). Over the past decade, a number of noteworthy observations have been made, including detections from 400 MHz (CHIME/FRB Collaboration et al. 2019a) to 8 GHz (Gajjar et al. 2018; Zhang et al. 2018), FRBs with extreme implied distances (Bhandari et al. 2018), and the repeating sources FRB 121102 (Spitler et al. 2016) and FRB 180814 (CHIME/FRB Collaboration et al. 2019b). The source FRB 121102 has been associated with a dwarf galaxy at redshift $z = 0.19$ (Marcote et al. 2017) and shows extreme Faraday rotation (Michilli et al. 2018), demonstrating that it is situated in a dense region in its host galaxy.

FRBCAT^a (Petroff et al. 2016) provides an up-to-date catalogue of reported FRB detections with 65 reported FRBs at the time of writing this paper. Recently, there has been a significant increase in the number of reported FRBs as new wide field of view (FoV) arrays have begun operating. The Australian Square Kilometre Array Pathfinder (ASKAP), when observing in ‘fly’s eye’ mode to maximise sky coverage, has detected 25 FRBs (Macquart et al. 2019; Qiu et al. 2019; Bhandari et al. 2019). Initial observations with Canadian Hydrogen Intensity Mapping Experiment (CHIME) have also resulted in 13 FRB detections (CHIME/FRB Collaboration et al. 2019a) including the repeating source FRB 180814 (CHIME/FRB Collaboration et al. 2019b).

Prior to ASKAP and CHIME, most of the FRBs were detected with the 64-m Parkes radio telescope. Only two FRBs have been detected with the Robert C. Byrd Green Bank Telescope (GBT). The first, FRB 110523 (Masui et al. 2015), was detected in archival GBT data acquired with the prime focus 800-MHz receiver (700–900 MHz). This detection—with a telescope other than Parkes—provided strong evidence that FRBs were in fact astrophysical. Recently, multiple bursts from the repeating source FRB 121102 were detected (Gajjar et al. 2018; Zhang et al. 2018) using the GBT C-Band (4–8 GHz) receiver, while the Green Bank Northern Celestial Cap (GBNCC) Pulsar Survey at 350 MHz reported a non-detection of FRBs (Chawla et al. 2017). Recently, Golpayegani and

Author for correspondence: Mayuresh P. Surnis, Email: mayuresh.surnis@mail.wvu.edu

Cite this article: Surnis MP, Agarwal D, Lorimer DR, Pei X, Foster G, Karastergiou A, Golpayegani G, Maddalena RJ, White S, Armour W, Cobb J, McLaughlin MA, MacMahon DHE, Siemion APV, Werthimer D and Williams CJ. GREENBURST: A commensal Fast Radio Burst search back-end for the Green Bank Telescope. *Publications of the Astronomical Society of Australia* 36, e032, 1–6. <https://doi.org/10.1017/pasa.2019.26>

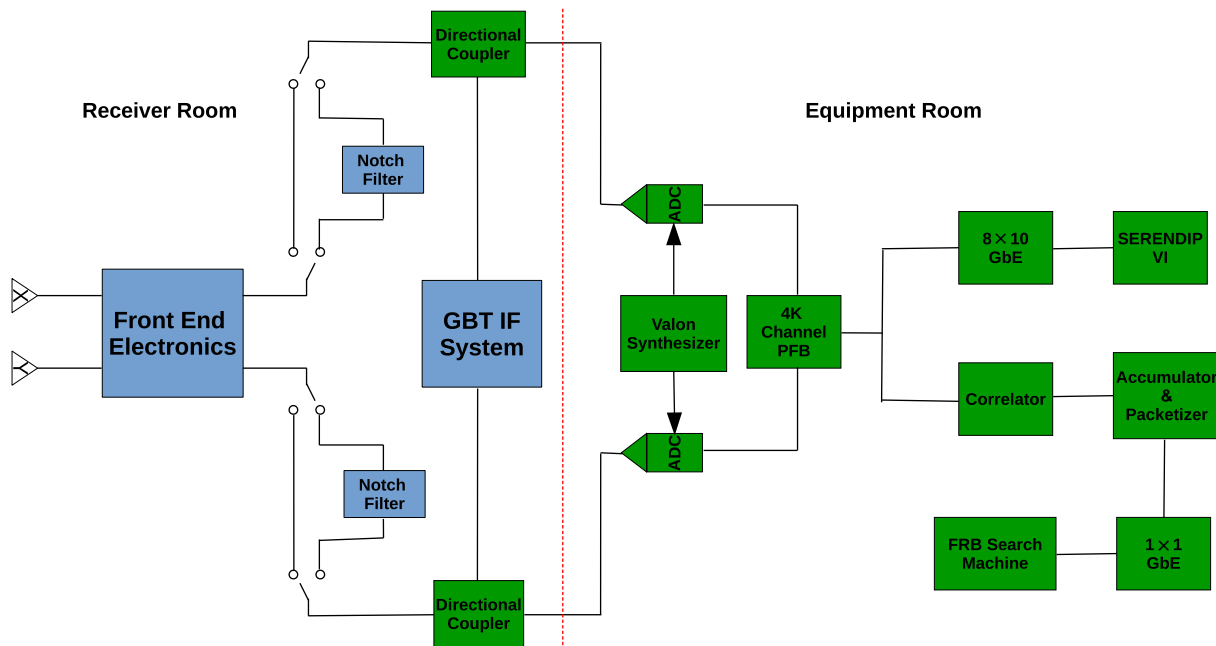


Figure 1. Block diagram showing the signal chain for the regular (blue components) and commensal mode (green components) for the L -band receiver. The signal chain on the left of the dashed red line is located in the receiver room, while the chain on the right is located in the equipment room. The signal travels on an optical fibre from the receiver room to the equipment room.

Lorimer (2019) also reported non-detection of FRBs at L -band using the 20-m telescope on the GBT site.

Wide FoV arrays have been very successful in detecting FRBs, but there still exists a strong motivation for using high-gain, single-element telescopes for FRB surveys. Though the GBT has a narrow FoV compared to that of ASKAP or Parkes, the GBT provides a significant increase in sensitivity [a fluence limit of 0.325 Jy ms as compared to 22 Jy ms for ASKAP (Bhandari *et al.* 2019) and 0.9 Jy ms for Parkes (Thornton *et al.* 2013)]. See Section 4 for detailed calculations], allowing for the detection of low-fluence FRBs that would otherwise be missed. These detections would provide an important contribution to future population studies.

Based on previous detections,^b FRBs show no preferred sky direction. As such, commensal data acquisition systems provide augmented science output from an observation at the additional cost of running dedicated hardware (Foster *et al.* 2018). For a fixed FoV, maximising the total observing time also maximises the event detection rate. A dedicated splitter for the L -band receiver was recently installed on the GBT. This allows for full-time observations using this receiver even when other receivers are at the Gregorian focus. These observations at lower, but still reasonable, sensitivity still provide vital time on the sky, hence maximising the possibility of an FRB detection.

In this work we discuss the design and implementation of the commensal FRB search back-end using the dedicated L -band tap. We discuss the signal path and processing pipeline in Section 2. Initial test observations to verify the pipeline are covered in Section 3. We also discuss the survey sensitivity and expected detection rates in Section 4.

2. System description

GREENBURST is inspired from its predecessor at the Arecibo Telescope, SETIBURST, and works in parallel with a duplicate

SERENDIP VI system, which is a high performance compute system recording spectra at a time resolution of 1.198 s for the purpose of searching for extraterrestrial signals (see Chennamangalam *et al.* 2017, for more details). Although the concept for GREENBURST is derived from SETIBURST, it differs in implementation significantly. The back-end consists of three sub-systems, the commensal modifications at the front-end, the ROACH2 Field Programmable Gate Array (FPGA) board^c for signal processing, and an FRB search system. We describe each of these in the subsections below.

2.1. L -band receiver commensal modifications

The GBT has an unblocked aperture with an off-axis arm containing an eight-position feed turret. The front-end analogue electronics are situated below a secondary reflector, 8 m in diameter. A circular turret with eight positions is used to select the primary observing receiver. In an earlier test, Maddalena (2013) found that apart from the focus position, the L -band (1–2 GHz) feed can be used for commensal observing in four more positions with decreasing sensitivity relative to the focus position. We have added a directional coupler to the L -band feed to allow commensal mode observations even when the feed is not being used as the primary observing feed.

The dual-polarisation L -band Radio Frequency (RF) signal received from the feed (denoted as X and Y in Figure 1) travels through the front-end electronics which consists of an optional circular polarisation synthesiser, Low-Noise Amplifier (LNA), noise calibrator, and a user-selectable notch filter.^d We installed two directional couplers (one for each of the polarisations) with 20 dB gain in the L -band signal chain between the notch filter and the intermediate frequency (IF) system (see Figure 1).

^c<https://casper.berkeley.edu/wiki/ROACH2>.

^dThe notch filter is a user-selectable filter to suppress a known radar signal in the frequency band between 1 200 and 1 310 MHz

^b<http://frbc.org>.

The output from the coupler is then transmitted to the equipment room through an optical fibre and digitised. We added isolators before the couplers to minimise reflections which were inducing ripples across the receiver bandpass.

We then conducted tests to ensure that the additional components do not affect regular observations. In these tests, we observed in the direction of the North celestial pole at night, under good weather. This reduced the possibility of introducing changes in spillover from ground, elevation/atmosphere, the sky, and baseline shapes from standing waves in the optics due to solar illumination. We conducted a 11-min observation using the digital continuum receiver (DCR) to cover the entire *L*-band frequency range of 1 150–1 730 MHz. The addition of the coupler resulted in a negligible change in system temperature. We also conducted 40-min observations in the single window spectral mode at centre frequencies of 1 365, 1 400, 1 420, and 1 665 MHz with a bandwidth of 20 MHz to ensure that the spectral-line data quality did not suffer due to the insertion of the couplers. We concluded that the insertion of the couplers in the signal chain did not degrade the data quality. Although we did not specifically conduct tests, there have been regular pulsar timing observations carried out by the North American Nanohertz Observatory for Gravitational Waves (NANOGrav), confirming that our system does not affect pulsar timing observations. We also carried out test observations on PSR B0329+54 in the search mode with the Green Bank Ultimate Pulsar Processing Instrument (GUPPI) simultaneously to confirm that the search mode observations do not get affected by our system.

2.2. Modified SERENDIP VI FPGA design

A ROACH2 board is used to perform digital signal processing (DSP) on the *L*-band signal. This board is primarily used for the SERENDIP VI system (see Chennamangalam et al. 2017, for more details) but we have updated the firmware with additional capabilities for GREENBURST. The analogue signal is digitised with an 8-bit Analog-to-Digital Converter (ADC) at 1 920 million samples per second. A Valon frequency synthesiser is used as the sampling clock. The second Nyquist zone is used to sample the 960–1 920 MHz band. A polyphase filterbank (PFB) is used to channelise the band into 4 096 frequency sub-bands. The sub-bands are then power detected and accumulated to produce a spectrum every 256 μ s (see Figure 2 for an example). The spectrum is then packetised and transmitted as User Datagram Protocol (UDP) packets over a 1 Gb Ethernet link to the FRB search machine. A complete spectrum is divided into 16 packets. Each packet contains 256 spectral channels for each polarisation with a total of 768 bytes of data (256 bytes header, 256 bytes power of *X*, and 256 bytes power of *Y*). This results in a data rate of 384 Mbps. Due to hardware limitations, we are currently not storing any polarisation information, but plan to do so in the future. The modified FPGA design is publicly available for download.^e

2.3. FRB search machine

The FRB search machine is composed of two Intel Xeon E5–2640 processors, an NVIDIA GeForce GTX Titan Xp graphics processing unit (GPU) with Pascal architecture and 12 GB memory, a 1.2 TB solid-state drive for temporary storage, and a 10 TB additional hard drive for long-term storage.

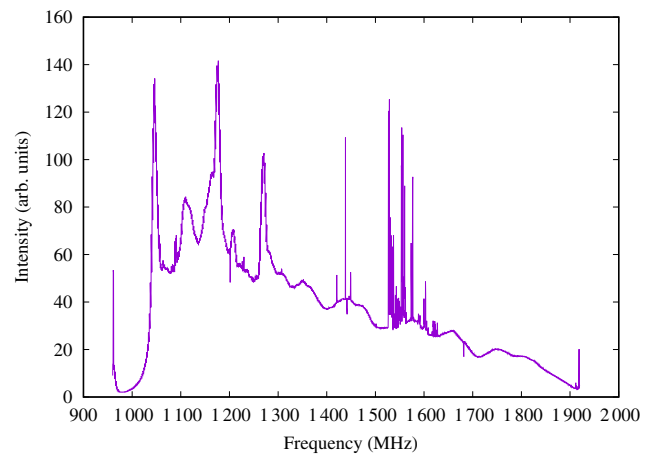


Figure 2. Bandpass response of the GREENBURST system from an observation carried out when the *L*-band feed was at the Gregorian focus. The bandpass shape is similar at other turret positions but with noise statistics proportional to T_{sys} .

We use a custom receiver code^f to capture the incoming UDP packets and reconstruct the spectra. To do this, we use two static buffers, each of length 2^{17} samples. This corresponds to 33.6 s of time, which is the dispersion delay across our band at a DM of $10\,000\text{ pc cm}^{-3}$. The static buffers are used in an alternate fashion, i.e., at a given time, one buffer is used to save a copy of the incoming spectra while the other is used to write the previous data block to disk. The code writes 2^{21} spectra (corresponding to an integration time of ~ 537 s) to a single filterbank file. In order to avoid losing candidate information in the last data block, we have implemented an overlap of 33.6 s between two consecutive filterbank files. Once a filterbank file is created, the search pipeline carries out a single-pulse search covering a Dispersion Measure (DM) range of $10\text{--}10\,000\text{ pc cm}^{-3}$. This search is performed using the GPU-accelerated HEIMDALL^g program. The pipeline then sifts through potential candidates and produces plots for most likely FRB candidates. Further details of the completed pipeline will be discussed in a future paper.

3. Initial observations and sensitivity tests

We measured the sensitivity of GREENBURST by switching between the eight turret feed positions and observing the same calibrator source. We measured the effective system temperature T_{sys} for the *L*-band receiver using the DCR at 1 375 MHz with a 20 MHz bandwidth and a sampling time 200 ms to observe the calibrator source 3C147 (see Figure 3 for an example). The additional noise ΔT_{sys} due to the turret position offset (relative to the *L*-band feed at the focus) is plotted as black dots in Figure 4 and listed in Table 1. The beam shape of the feed is slightly broadened at the offset turret positions due to axial de-focusing. We measured this for each turret position using the calibrator scans. We list the turret frame offsets and measured FoV (equivalent width at the half power point) of the *L*-band feed in Table 1. Observing with the *L*-band feed when in neighbouring turret positions (*C*-band, MUSTANG) results in approximately 30% decrease in sensitivity. In the worst case, when the *S*-band feed is at the focus, the effective sensitivity of the *L*-band system is equivalent to a single dish with a diameter of about 28 m.

^e<https://github.com/SparkePei/dibas-upgrade-frb>.

^f<https://github.com/mpsurnis/greenburst>.

^g<https://sourceforge.net/projects/heimdall-astro>.

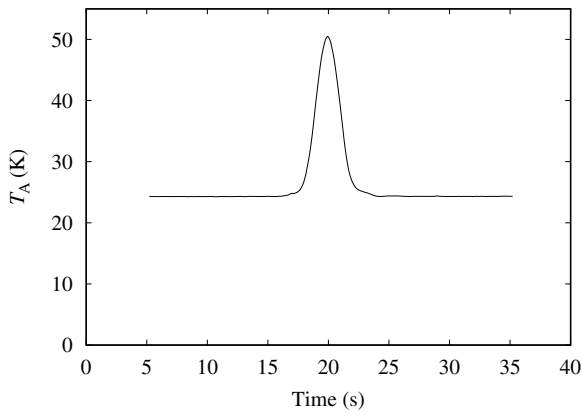


Figure 3. Antenna temperature (T_A) as a function of time for a continuum scan across 3C147 at turret position 2. The baseline offset is caused by the sky background and excess system noise (ΔT_{sys}) due to the offset from secondary focus.

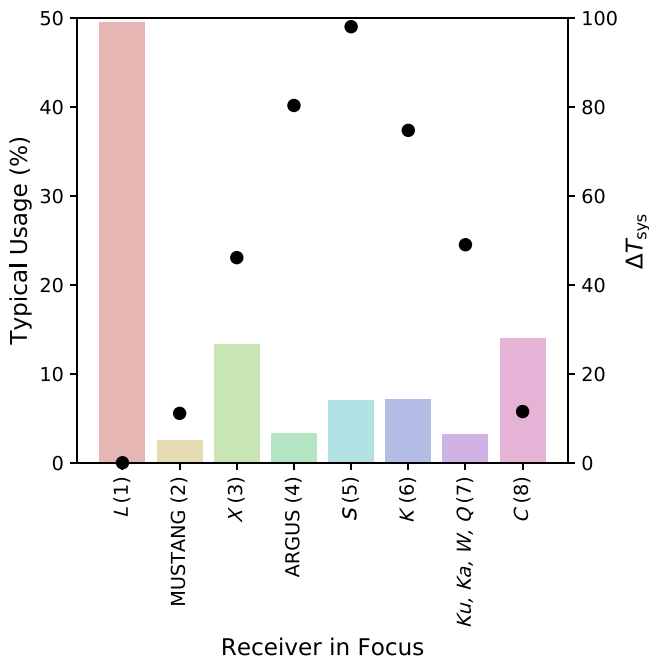


Figure 4. Excess system temperature ΔT_{sys} as a function of the receiver in focus/turret position for the GBT L -band receiver (black points). Expected typical receiver usage based on 2018 usage (bars).

Extended prime focus feed blocks the secondary reflector, making commensal observations impossible. Thus, we would not be observing with GREENBURST during prime focus observations.

To test the FRB search pipeline, we observed PSR B0329+54. An example candidate plot from the real-time single pulse search pipeline is shown in Figure 5. Our single-pulse search pipeline will produce similar plots for all the potential FRB candidates.

Figure 4 also shows the typical percentage usage of the feeds based on 2018 usage statistics (T. Minter, private communication). Turret positions 4 (ARGUS), 5 (S-band), and 6 (K-band) are partially blocked by the primary focus structure resulting in significantly reduced sensitivity. But, only approximately 15% of the 2018 observing time was used for observations with these feeds. Nearly half of the observing time was using the L -band feed, and as such most GREENBURST observations will be at the optimal sensitivity.

4. Event rate predictions

To estimate the expected FRB rate with GREENBURST, we first use the radiometer noise considerations to compute the minimum detectable flux density

$$S_{\text{min}} = \frac{S/N_{\text{min}} T_{\text{sys}}}{G \sqrt{n_p t_{\text{obs}} \Delta f}}, \quad (1)$$

where we assume a system temperature (T_{sys}) of 40 K (including a cold sky temperature of 10 K), a cut-off signal to noise ratio (S/N) of 10 (S/N_{min}), telescope gain (G) of 2 K Jy^{-1} , with two polarisations summed ($n_p = 2$) over a bandwidth (Δf) of 960 MHz, and a typical FRB pulse width (t_{obs}) of 5 ms. This results in an S_{min} of 65 mJy at the bore-sight or 130 mJy at the half power point of the beam. Rearranging Equation (6) from Lawrence et al. (2017), replacing a by R_0 and b by α , above a flux density S , we get the expected FRB rate:

$$R(> S) = \frac{\pi r^2}{\alpha \ln(2)} R_0 \left(\frac{S}{1 \text{ Jy}} \right)^{-\alpha}, \quad (2)$$

where R_0 is the all-sky rate of FRBs and α is the (currently uncertain) slope of the source count distribution. For a population of sources uniformly distributed in Euclidean space, $\alpha = 1.5$. We have also assumed a circular beam with a Gaussian power pattern with r being the half width at half maximum. Adopting a value of 4.6 arcmin for r (see Table 1), 0.91 for α , and a maximum sky rate R_0 of 924 FRB events per sky per day (Lawrence et al. 2017) results in a maximum rate of 5×10^{-2} FRB events per day for GREENBURST. Inverting the rate gives us the minimum wait time of 20 d before the first FRB detection. Figure 6 shows the ranges of the wait times based on the 95% confidence intervals on α and R_0 as reported by Lawrence et al. (2017). For a mean value of 0.91 for α and 587 FRB events per sky per day for R_0 (as reported by Lawrence et al. 2017), we get a mean wait time of 32 d of continuous operation at the Gregorian focus (turret position 1) for GREENBURST. Using the method described above, we have estimated S_{min} and the projected FRB rates for other turret positions in Table 1. We expect a combined expected FRB rate of 2–7 per year of operation.

5. Discussion

We have estimated the wait time for the first FRB detection adopting the all-sky rate from Lawrence et al. (2017). Based on the usage statistics for the GBT in the year 2018, the L -band feed was used for scientific observations for approximately 2970 h out of a total of about 7125 h of on-sky time (T. Minter, private communication). For the 95% confidence interval range of the all-sky FRB rates (Lawrence et al. 2017), we project that GREENBURST would detect between 2 and 6 FRBs per year. This rate estimate includes the time L -band used at the Gregorian focus. The adjacent turret positions (positions 2 and 8) constitute an additional 1000 h of observing time. With a 11 K excess ΔT_{sys} , this would result in one additional FRB per year. The remaining time at other turret positions may result in more serendipitous detections, especially of low-DM and high-brightness events such as the recently discovered ASKAP (Shannon et al. 2018) and CHIME (CHIME/FRB Collaboration et al. 2019a) FRBs. Given this rate, even a non-detection would be useful in constraining the value of α towards the higher end in Figure 6. Assuming that 2018 usage indicates typical GBT usage, we get about 123 d of observations at the maximum sensitivity. Even if half of these data are corrupted by Radio-frequency Interference (RFI), a non-detection would exclude all

Table 1. A summary of the relevant parameters for all GBT turret positions. From left to right, the columns list turret position, feeds currently in position, approximate turret rotation angle corresponding to the position offset from the *L*-band position, the offsets in azimuth (ΔAz) and elevation (ΔEl), the excess system temperature ΔT_{sys} for the *L*-band receiver as compared to the focus position, the measured FoV of the telescope beam, the antenna temperature (T_A), aperture efficiency (η), telescope gain (G), estimated sensitivity at the half-power point (S_{min}), usage based on total on-sky time in 2018, and our estimated FRB rate (see text).

Turret position	Receiver	Rotation angle (°)	ΔAz (arcmin)	ΔEl (arcmin)	ΔT_{sys} (K)	FoV (arcmin)	T_A (K)	η	G (K/Jy)	S_{min} (Jy)	Usage (%)	FRB rate (yr^{-1})
1	<i>L</i> -band	0	0.0	0.0	0.0	9.2	37.45	0.70	2.0	0.130	41.7	2–6
2	MUSTANG	300	22.5	−13.2	11.1	9.4	28.06	0.52	1.4	0.236	2.1	0.05–0.2
3	<i>X</i> -band	260	25.3	−30.2	46.1	9.5	14.01	0.26	0.7	0.794	11.2	0.1–0.3
4	ARGUS	220	16.2	−45.7	80.3	10.8	8.26	0.15	0.4	1.936	2.8	0.01–0.04
5	<i>S</i> -band	180	0.0	−51.5	98.0	10.8	4.28	0.08	0.2	4.454	5.9	0.01–0.04
6	<i>K</i> -band	140	−16.9	−45.2	74.7	10.3	6.97	0.13	0.4	1.856	6.0	0.02–0.08
7	<i>Ku</i> -band ^a	100	−25.4	−29.8	49.0	9.6	14.94	0.28	0.8	0.718	2.7	0.02–0.08
8	<i>C</i> -band	60	−22.1	−12.5	11.5	9.3	28.84	0.54	1.5	0.224	11.8	0.3–1.0

^aTurret position 7 also houses *Ka*-band, *W*-band, and *Q*-band feeds in rotation.

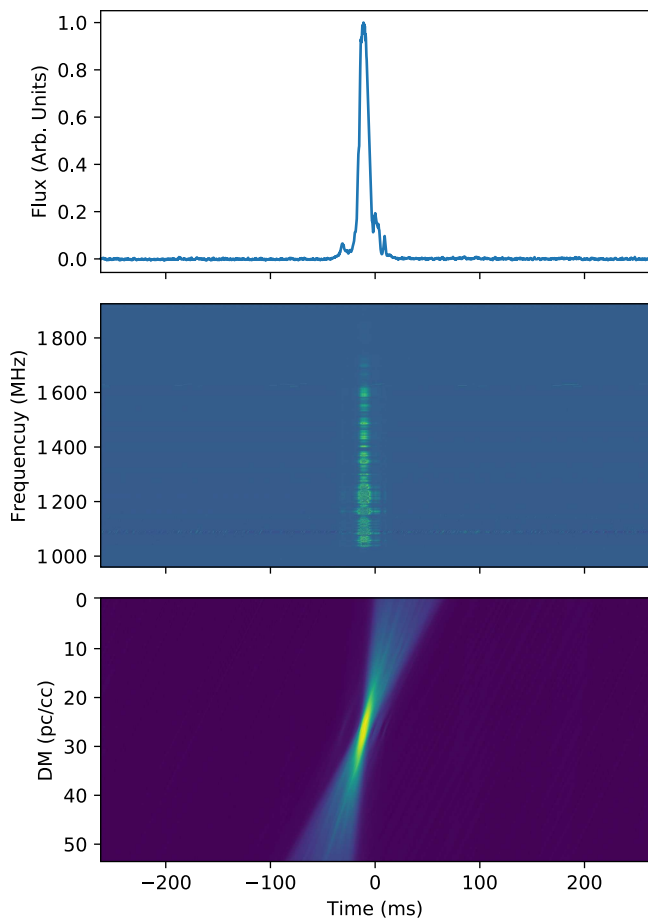


Figure 5. Candidate plot showing a single pulse detected from PSR B0329+54 with the GREENBURST pipeline. Top panel shows the pulse in time, middle panel shows the de-dispersed pulse as a function of frequency, and the bottom panel shows the pulse in DM-time plane.

values of $\alpha > 1$. It was recently noticed that the estimated value of α is inconsistent between Parkes and ASKAP (James et al. 2019). An independent estimation of α with the GBT is critical for constraining the all-sky FRB rate. A limited number of detections in the first year would also help putting useful constraints on the values of R_0 , which is the instrument-independent all-sky FRB rate. Thus, GREENBURST is a promising FRB instrument regardless of the outcome.

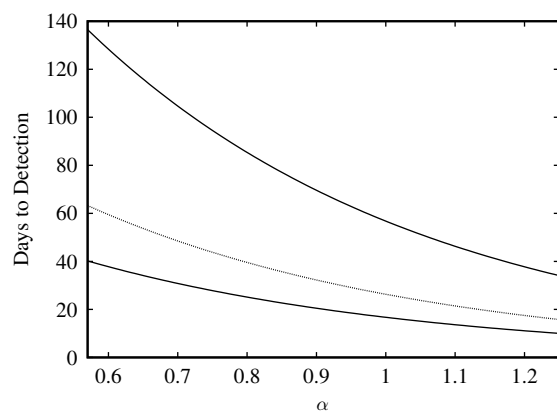


Figure 6. Predicted number of days to the first FRB detection with GREENBURST as a function of α . The dotted line in the middle denotes the mean, while the dot-dashed lines denote the 95% confidence intervals

Most current FRB back-ends search multiple beams (e.g. ASKAP, CHIME, Parkes, and ALFABURST), while GREENBURST is a single-beam survey. Although this reduces sky coverage, the high sensitivity of the GBT still means it has the potential to detect FRBs. This increases the search volume in redshift and thus compensates for the lack of sky coverage. If a repeating FRB was detected with GREENBURST, the narrow telescope beam would reduce the prospective sky area for follow-up observations. This would speed-up the identification of the host galaxy associated with the FRB.

The typical *L*-band bandpass (Figure 2) shows a lot of RFI in some parts of the band. We usually flag all the frequency channels that are corrupted by RFI by using a median-based filter. The *L*-band feed of the GBT is used primarily for spectral line observations. During these observations, there is usually a flickering diode that injects noise at a fixed level. The noise injection takes place in the form of a square wave pattern with variable frequency and duty cycle. We have tested our pipeline along with different settings of the noise diode (as set by the then current observer) to ensure that the noise diode does not produce spurious FRB candidates. The single-pulse pipeline has many more features, and we plan to discuss those in more detail in a separate paper in the future.

The GREENBURST pipeline will carry out a blind search for single-pulses over a large DM range. This range includes Galactic DMs as well. Thus, in addition to FRBs, our pipeline

may also discover radio transients in our Galaxy. The distinct advantage provided by the commensal mode observing is that GREENBURST would be recording data all the time, enabling it to make serendipitous discovery of a Galactic radio transient. We have already made such a discovery with the ALFABURST while the telescope was slewing between targets (Foster *et al.* 2018). Regarding the detection probability during slewing, we would like to make a note. At the maximum slew rate of about 40 degree per minute of the GBT, we would not be able to detect any source above a DM of 71 pc cm^{-3} in the whole band, while for a detection in half of the band, the corresponding DM is about 274 pc cm^{-3} . Thus, the probability of detecting a Galactic transient is greater during slewing. In addition, GREENBURST may detect more radio pulses from known rotating radio transients (RRATs).^h

We have a working pipeline, and at the time of writing have acquired data for a week. We are currently carrying out data quality checks and tuning our search pipeline to the observed RFI in the data. We are also ascertaining whether all the metadata are properly logged by cross-referencing them with the GBT logs. GREENBURST is exiting its commissioning phase and will soon start searching for FRBs in real-time.

Acknowledgements. We thank West Virginia University for its financial support of GBT operations, which enabled some of the observations for this project. M.P.S., M.A.M., and D.R.L. acknowledge support from NSF RII Track I award number OIA-1458952. M.P.S., M.A.M., G.G., and D.R.L. are members of the NANOGrav Physics Frontiers Center which is supported by NSF award 1430284. Berkeley efforts were supported by NSF grants 1407804 and 1711254, as well as the Marilyn and Watson Alberts SETI Chair funds. The Green Bank Observatory is a facility of the National Science Foundation operated under cooperative agreement by Associated Universities, Inc.

References

- Bhandari, S., *et al.* 2018, *MNRAS*, **475**, 1427
- Bhandari, S., Bannister, K. W., James, C. W., Shannon, R. M., Flynn, C. M., Caleb, M., & Bunton, J. D. 2019, *MNRAS*, **486**, 70
- CHIME/FRB Collaboration, *et al.* 2019a, *Nature*, **566**, 230
- CHIME/FRB Collaboration, *et al.* 2019b, *Nature*, **566**, 235
- Chawla, P., *et al.* 2017, *ApJ*, **844**, 140
- Chennamangalam, J., *et al.* 2017, *ApJS*, **228**, 21
- Foster, G., *et al.* 2018, *MNRAS*, **474**, 3847
- Gajjar, V., *et al.* 2018, *ApJ*, **863**, 2
- Golpayegani G., *et al.* 2019, arXiv e-prints, [arXiv:1905.00980](https://arxiv.org/abs/1905.00980)
- James, C. W., Ekers, R. D., Macquart, J.-P., Bannister, K. W., & Shannon, R. M. 2019, *MNRAS*, **483**, 1342
- Lawrence, E., Vander Wiel, S., Law, C., Burke Spolaor, S., & Bower, G. C. 2017, *AJ*, **154**, 117
- Lorimer, D. R., Bailes, M., McLaughlin, M. A., Narkevic, D. J., & Crawford, F. 2007, *Sci*, **318**, 777
- Macquart, J.-P., Shannon, R. M., Bannister, K. W., James, C. W., Ekers, R. D., & Bunton, J. D. 2019, *ApJ*, **872**, L19
- Maddalena, R. J. 2013, Technical Report 285, Properties of the GBT at L-band for Commensal Observing. https://library.nrao.edu/public/memos/gbt/GBT_285.pdf. NRAO, Green Bank, WV, https://library.nrao.edu/public/memos/gbt/GBT_285.pdf
- Marcote, B., *et al.* 2017, *ApJ*, **834**, L8
- Masui, K., *et al.* 2015, *Nature*, **528**, 523
- Michilli, D., *et al.* 2018, *Nature*, **553**, 182
- Petroff, E., *et al.* 2016, *PASA*, **33**, e045
- Qiu, H., Bannister, K. W., Shannon, R. M., Murphy, T., Bhandari, S., Agarwal, D., Lorimer, D. R., & Bunton, J. D. 2019, *MNRAS*, **486**, 166
- Shannon, R. M., *et al.* 2018, *Nature*, **562**, 386
- Spitler, L. G., *et al.* 2016, *Nature*, **531**, 202
- Thornton, D., *et al.* 2013, *Sci*, **341**, 53
- Zhang, Y. G., Gajjar, V., Foster, G., Siemion, A., Cordes, J., Law, C., & Wang, Y. 2018, *ApJ*, **866**, 149

^h<http://astro.phys.wvu.edu/rratalog>.